nature physics

INSIGHT | REVIEW ARTICLES

PUBLISHED ONLINE: 1 OCTOBER 2010 | DOI: 10.1038/NPHYS1797

Physical virology

W. H. Roos[1]*, R. Bruinsma[2] and G. J. L. Wuite[1]*

Viruses are nanosized, genome-filled protein containers with remarkable thermodynamic and mechanical properties. They form by spontaneous self-assembly inside the crowded, heterogeneous cytoplasm of infected cells. Self-assembly of viruses seems to obey the principles of thermodynamically reversible self-assembly but assembled shells ('capsids') strongly resist disassembly. Following assembly, some viral shells pass through a sequence of coordinated maturation steps that progressively strengthen the capsid. Nanoindentation measurements by atomic force microscopy enable tests of the strength of individual viral capsids. They show that concepts borrowed from macroscopic materials science are surprisingly relevant to viral shells. For example, viral shells exhibit 'materials fatigue' and the theory of thin-shell elasticity can account — in part — for atomic-force-microscopy-measured force–deformation curves. Viral shells have effective Young's moduli ranging from that of polyethylene to that of plexiglas. Some of them can withstand internal osmotic pressures that are tens of atmospheres. Comparisons with thin-shell theory also shed light on nonlinear irreversible processes such as plastic deformation and failure. Finally, atomic force microscopy experiments can quantify the mechanical effects of genome encapsidation and capsid protein mutations on viral shells, providing virological insight and suggesting new biotechnological applications.

The impact of viruses on our daily lives is dominated by their role as infectious agents of, often serious, diseases. However, viruses are now increasingly employed in more positive roles[1,2]. Examples include viruses and viral shells that are used in batteries and memory devices[3,4], as nanoscaffolds or nanoreactors for transport and catalysis[5,6], and in cancer treatment[7]. In the context of gene therapy, they are used as vectors for gene delivery[8], and the 'phage' viruses that infect bacteria have been used as antibacterial agents[9]. Supporting these applications is the burgeoning research field of physical virology dedicated to the study of the physical properties of viruses[10]. It encompasses domains such as viral self-assembly[11,12], virus genome packaging and release mechanisms[13–15], and structural and mechanistic studies of viral particles[14,16,17]. The rapid growth of this field is, on the one hand, fuelled by the development of physics-based techniques such as cryo-electron microscopy, X-ray crystallography, optical tweezers and atomic force microscopy and, on the other hand, by the increasing interest in viral particles as 'smart' building blocks of larger-scale structures. In this brief review we shall focus on just two aspects of physical virology: first what physics has to tell us about the assembly of viral shells, and second what the mechanical properties of assembled viral shells are: how we can experimentally probe mechanical properties of viral shells, how we should interpret them and how we can apply the insights these studies provide.

Viral self-assembly

Viruses do not carry out metabolic activity and rely entirely on host-cell molecular machinery for reproduction. This absence of metabolic and reproductive activity suggests that, unlike cells, the assembly of viruses could perhaps be understood on the basis of equilibrium thermodynamics. An elegant confirmation of this idea was the discovery in 1955 by Fraenkel-Conrat and Williams[18,19] that under *in vitro* conditions the rod-like tobacco mosaic virus (TMV) self-assembles spontaneously and unassisted into fully infectious viral particles from solutions containing the molecular components of this virus: the TMV capsid proteins (or 'subunits') and the single-stranded (ss) RNA genome molecules of TMV. In 1967, Bancroft, Hills and Markham[20] showed that small sphere-like plant viruses with icosahedral symmetry also can be produced by *in vitro* self-assembly (Box 1 summarizes the general classification of viruses with icosahedral viral symmetry). The connection between equilibrium thermodynamics and viral self-assembly was further strengthened by the work of Klug[21], who determined the thermodynamic phase diagram of solutions of TMV subunits in terms of acidity and salinity. Capsid proteins, or 'subunits', interact mainly through a combination of electrostatic repulsion, hydrophobic attraction and specific contacts between certain pairs of amino acids (known as 'Caspar pairs'[22]). Varying the acidity and salinity conditions (or the concentration of Ca^{2+} ions) adjusts the relative balance between these competing interactions, thereby favouring assembly or disassembly[23] of protein aggregates. For TMV subunits in ambient conditions of acidity–salinity–temperature the most stable subunit aggregates are 'double-disc' and 'double-ring' protein clusters held together by hydrophobic attractive interactions. Electrostatic repulsion between the positively charged discs/rings prevents disc aggregation. The addition of the oppositely charged ssRNA genome molecules drives the self-assembly process to completion by combining the protein discs into rod-like cylinders with the RNA molecule running along the central axis, like beads on a string[21]. Self-assembly of most infectious sphere-like ssRNA viruses under ambient conditions requires the presence of the viral RNA genome molecules. Viral RNA molecules act in part as a non-specific 'electrostatic glue' that links together the oppositely charged capsid proteins[24], and particular 'stem-loop' side branches of the RNA molecules have specific affinity for the capsid proteins. In some cases, the encapsidated ssRNA molecules condense as double-stranded (ds) helical segments along a dodecahedral cage of edges of the icosahedral shell[25]. Self-assembly of empty capsids in the absence of RNA may be possible as well for certain viruses, for instance under non-ambient pH or salinity levels. On the other hand, self-assembly of viral shells of most ds genomes, such as the tailed dsDNA 'bacteriophage' viruses (that is, viruses that prey on bacteria), does not require the presence of genome molecules. The much larger bending rigidity of dsDNA molecules presumably prevents them from acting as 'electrostatic glue'.

[1]Natuur- en Sterrenkunde & Laser Centrum, VU University, De Boelelaan 1081, 1081 HV Amsterdam, The Netherlands, [2]Department of Physics, University of California, Los Angeles, California 90095-1537, USA. *e-mail: wroos@few.vu.nl; gwuite@nat.vu.nl.

Box 1 | Viral shapes.

Viral particles come in many shapes, of which sphere-like and rod-like particles are the most common, but spherocylinders, cones and other shell shapes are seen as well. About half of all viral families share icosahedral symmetry, even when the viral genomes share little homology[92]. Examples include the plant virus CCMV, the animal virus HBV and bacteriophage viruses discussed in this review. Caspar and Klug (CK) developed a classification system for icosahedral viruses, illustrated in Fig. B1, based on the 'T number' defined as $T = m^2 + n^2 + mn$. Here, m and n indicate the number of steps along the crystallographic directions of a hexagonal lattice connecting two adjacent vertices on the icosahedron[93,94]. A CK icosahedral shell consists of 12 pentamers located at equidistant sites on the icosahedral vertices with a further $10(T-1)$ hexamers — with $T = 1, 3, 4, 7, \ldots$ — located in between the pentamers. Following earlier work by Crick and Watson[95], CK argued that this type of icosahedral shell minimizes the geometrically unavoidable elastic strains of identical proteins placed on a closed shell ('quasi-equivalence').

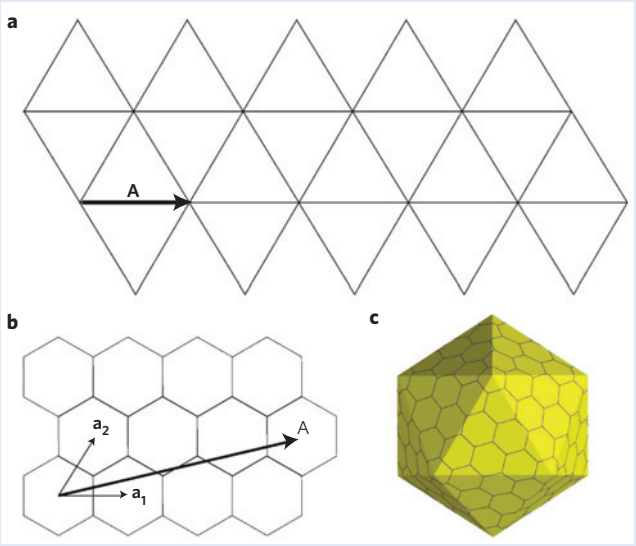

Figure B1 | Caspar and Klug construction of icosahedral viral shells. **a**, Template — consisting of equilateral triangles — of which an icosahedron can be folded. The lattice vector $\mathbf{A} = m\mathbf{a_1} + n\mathbf{a_2}$ of a hexagonal lattice with basis vectors $\mathbf{a_1}$ and $\mathbf{a_2}$ forms an index for the triangles. **b**, An example for $m = 3$ and $n = 1$. **c**, Result of folding a template with this lattice vector into an icosahedron. It has a $T = m^2 + n^2 + mn = 13$ structure with $10(T-1) = 120$ hexamers in total. Reproduced with permission from ref. 48, © 2005 APS.

In these cases, the genome is usually inserted, after capsid assembly has been completed, by the action of a rotary molecular motor imbedded in the capsid[15].

Assembly studies by the group of Zlotnick of the assembly of two icosahedral viruses — cowpea chlorotic mottle virus (CCMV; ref. 26) and hepatitis B virus (HBV; ref. 27) — were an important milestone for the application of equilibrium thermodynamics. They measured the concentrations of subunit clusters of different sizes as a function of the total protein concentration and encountered a double-peaked population composed of, respectively, small clusters (for example, dimers or pentamers) and fully formed capsids. The surprise was that the ratio of the concentrations of free subunits and fully formed capsids seemed to obey quantitatively the law of mass action (LMA). The LMA would demand that for a viral shell composed of N subunits the concentration of assembled capsids should be proportional to ϕ^N, with ϕ the concentration of free subunits, which must be distinguished from the total protein concentration ϕ_T. An important consequence of the LMA is the fact that, as a function of ϕ_T, the fraction $f(\phi_T)$ of proteins incorporated into capsids rises sharply at a quasi-critical concentration ϕ_{crit} with $f(\phi_T) \sim 1 - \phi_{crit}/\phi_T$ for $\phi_T > \phi_{crit}$. As, according to the LMA, the value of $\phi_{crit} \propto \exp(\beta \Delta G_0/N)$ is determined by the 'standard Gibbs free energy' ΔG_0 of the assembly reaction, that is, the assembly free energy of the capsid, important thermodynamic information can be obtained by measuring ϕ_{crit}. This form for $f(\phi_T)$ fits very well the equilibrium self-assembly curves of, for example, micelles ('critical micelle concentration')[28]. It describes quite well the self-assembly of CCMV and HBV with a ϕ_{crit} typically in the μM range. Under biological conditions, inside infected cells, the concentration of capsid proteins produced by transcription would thus have to exceed ϕ_{crit} before viral self-assembly could start. Fitted values for ΔG_0 were in the reasonable range of about $10\, k_B T$ per subunit, so in total about $10^3\, k_B T$ for small viral shells. The measured dependence of the fitted ΔG_0 on pH and salinity was also consistent with simple models for the interactions between subunits[23]. The LMA is a direct consequence of the minimization of the Gibbs free energy: it requires that capsid proteins in solution have the same chemical potential as the proteins incorporated in a shell. However, when the total concentration of capsid proteins is reduced back down below ϕ_{crit} after the assembly has reached completion, then capsids should disassemble spontaneously according to the LMA. In actuality this either does not happen at all, or happens only after a very long period of time, or after quite substantial changes in pH, salinity or other solution conditions[29]. This 'excess' thermodynamic stability of assembled viral shells when compared with conventional equilibrium self-assembly is, from a biological viewpoint, of course a prime 'survival' feature, as viral shells need to remain intact in 'hostile' environments that contain no free capsid proteins at all, such as the host bloodstream, stomach or tissue. This means that viral self-assembly really should not be viewed as an equilibrium process. Analytical and numerical studies[30] of simple models of capsid assembly kinetics[31] indicate that provided most assembly steps are reversible, with one or a few assembly steps irreversible, an LMA-type double-peaked distribution obeying $f(\phi_T) \sim 1 - \phi_{crit}/\phi_T$ will still develop under certain conditions. However, the 'ΔG_0' extracted from this ϕ_{crit} in general is considerably smaller than the actual standard free energy of the capsid, and reflects the assembly free energy of reversible intermediate structures.

Kinetic studies of viral self-assembly would be necessary to probe this limited form of irreversibility but, unlike the case of the rod-like TMV, it has turned out to be very challenging to identify experimentally the assembly intermediates of spherical viruses. Kinetic studies of viral assembly by electron microscopy carried out in the 1980s on brome mosaic virus (BMV) assembly reported partially formed shells[32]. In 1993, the group of Prevelige studied the kinetics of scaffold-based assembly of the phage P22 using light scattering[33]. Capsid assembly was shown to be preceded by a lag time after initiation followed by a more rapid sigmoidal growth curve, indicating that the capsid-assembly rate is determined by nucleation. A critical protein concentration is required below which assembly does not take place. The initial formation rate depended on the protein concentration to the fifth power, which suggests that in this case pentamers are the critical nuclei. RNA genome molecules have been shown to catalyse the assembly process by assisting the formation of the critical nucleus of BMV (ref. 34). Subsequent capsid growth seems to be sequential, resembling a polymerization reaction. Studies of the assembly kinetics of a number of viruses have reported similar scenarios, with lag times in the seconds–minutes range[35]. Particularly detailed was a multi-angle light-scattering study by

Casini *et al.*[36] of the assembly kinetics of human papilloma virus; they again found that the rate-limiting step of the assembly process was the formation of protein oligomers.

Numerical simulations of viral assembly kinetics could complement assembly-kinetics experiments. However, simulations on the relevant timescale of seconds to minutes that account for the internal degrees of freedom of capsid proteins interacting through realistic potentials are, for currently available computational resources, not practical. Instead, rigid geometrical models of the capsid proteins (or capsomeres) and other coarse-grained representations are used, with the model proteins/capsomeres interacting through some model pair potential[37–42]. In the simplest case, capsid proteins or capsomeres could even be represented as point particles. A Newtonian-dynamics study by Hagan and Chandler[41] of such a model reported that the choice of this pair potential sensitively determined whether 'kinetic traps' prevented proper assembly of small shells. Hicks and Henley[42] used an elastic model, with the proteins now represented as deformable triangles, and found that the probability for successful assembly of larger shells rapidly decreased when the elastic rigidity was increased. An example of an assembly error could be a five-fold-symmetric capsomere inserted at a location that is not appropriate for an icosahedral shell (see Box 1). More recently, molecular dynamics (MD) simulations of viral assembly have been carried out where the capsomeres/proteins were represented by more realistic geometrical shapes. MD simulations by Nguyen, Reddy and Brooks[43] were able to reproduce the self-assembly of smaller $T = 1$ and $T = 3$ shells. They found though that proper assembly was accompanied by the production of significant numbers of non-icosahedral 'aberrant' particles associated with assembly errors and kinetic traps, in particular when temperature and protein concentrations were not optimally chosen. Next, Rapaport[44] included explicit solvent molecules and succeeded in assembling $T = 1$ particles with a high level of fidelity and sigmoidal assembly kinetics. The high levels of assembly fidelity in this case seemed to be characterized by high levels of assembly reversibility. Recall that high levels of assembly reversibility were also required for the observed quasi-LMA. A 'local-rule' scheme has been proposed[45], engineered to prevent the assembly-error problem by assuming that viral proteins can adopt T different internal configurations 'coding' for proper assembly of an icosahedral shell with index T (see Box 1). So far, no evidence has been found for local-rule-based coding configurations.

If only the minimum-free-energy state of a shell is required then viral shell assembly also can be studied by Monte Carlo simulations. A 'two-disc' Monte Carlo simulation by Zandi *et al.*, representing pentamers and hexamers placed on a spherical support scaffold, found that the Caspar and Klug (CK) T-number icosahedral symmetry is indeed the minimum-free-energy structure provided that the size ratio of the discs is fixed appropriately[46]. Chen, Zhang and Glotzer[47] investigated cluster formation of attractive cone-shaped particles without support scaffold using Monte Carlo simulation. By varying the cone angle they found that the cones assembled into a sequence of convex shells characterized by 'magic numbers' that included the icosahedral shells. Non-icosahedral shell structures, like those of human immunodeficiency virus (conical) and of phage Φ29 (prolate/spherocylinder), can be obtained as minimum-energy structures for certain parameter ranges in elastic-shell models[48]. Design principles of prolate phages were reviewed by Moody[49] in 1999. Monte Carlo simulations of the packing of hard spheres on a prolate, spheroidal surface identified the minimal requirements to form shells resembling those of a few selected viruses[50], and Monte Carlo simulations of capsomere–capsomere interactions in prolate shells yielded optimal structures for particles with icosahedral end caps connected by cylinders of hexamers[51]. Finally, the capsids of many animal viruses, such as human immunodeficiency virus (HIV), HBV and herpes simplex virus, are surrounded by a lipid bilayer envelope, and Zhang and Nguyen studied the effect of this lipid bilayer on the nucleation of the cone-shaped HIV shells[52].

After the initial assembly of a virus, the capsid proteins are often modified, a process known as maturation. For example, the capsids of many tailed dsDNA bacteriophages undergo a whole sequence of conformational changes and chemical reactions that tend to strengthen the shell, which is necessary in part because of the large internal pressure of phages, which is discussed later on. The shell-maturation steps, which have been shown to be cooperative in certain cases, resemble structural phase transitions in crystals. The application of Ginzburg–Landau theory to describe the maturation steps indicates that near a step we could expect to encounter the same 'soft modes' as characterize structural transitions[53]. An exceptional case is the bacteriophage HK97, where, after an elaborate sequence of steps, the shell ends up being armoured by a cross-linked mesh of amino-acid chains that has the topology of medieval chain-mail[54]. Tama and Brooks[55,56] carried out all-atom numerical studies of some of the maturation steps of HK97 and found that the conformational changes of the shell do indeed tend to follow the trajectory of soft modes of the shell, associated with rotation of the pentamers and hexamers. Widom *et al.* used the continuum elasticity theory of thin shells to show that, even in the absence of internal protein conformational degrees of freedom driving the maturation, icosahedral shells should still exhibit soft modes near the buckling transition between spherical and icosahedral shapes[57]. Finally, Yang *et al.*[58] showed that the same theory could account for the low-frequency modes of the shells of simple viruses such as BMV.

Mechanical virology

After a virus or an empty viral shell has assembled, we can inquire how resilient it is in terms of its response to external force and other perturbations. Capsids need to meet conflicting demands: they should be sufficiently stable to protect their genome in the extracellular environment, but sufficiently unstable that they can release their genome molecules into host cells. Various bulk and single-particle assays have been developed to measure the mechanical properties of viruses, the budding field of mechanical virology. Osmotic-shock experiments were used to study the stability of bacteriophage viruses under pressure against rupture[14,59] and the mechanical properties of crystals and films composed of viruses were analysed by Brillouin light scattering[60,61]. A disadvantage of these multiparticle techniques is that (1) they represent an average over large numbers of viruses and (2) they represent a rotational average, so any directionality of the mechanical properties with respect to the shell orientation is lost. The mechanics of single particles and their directionality can however be probed with the atomic force microscopy (AFM-) based nanoindentation techniques summarized in Box 2.

The relation between the applied force and the resulting change in shell diameter is called the force–deformation curve (FDC; see Box 2). Depending on whether or not the capsid returns to its original state after the probe force is removed ('unloading'), we call this a reversible, respectively irreversible, deformation. The force measured by a nanoindentation probe results, at a fundamental level, from the fact that the probe forces the viral shell away from a state of minimum free energy. To interpret measured FDCs, including irreversibility effects, we can compare them with the deformation free energy obtained from the continuum elasticity theory of thin elastic shells ('thin-shell theory' or TST) that we have already mentioned. TST is used extensively by engineers to predict the effects of external forces on thin-walled, hollow macroscopic structures, such as aeroplanes or oil tanks. In the simplest application of TST we model a viral shell as a thin spherical

Box 2 | AFM nanoindentation.

The mechanical properties of various biological entities have been characterized by AFM-based nanoindentation[96], including cells[97,98], microtubules[99,100], peptide nanotubes[101] and viruses[67,79]. Figure B2 shows a schematic diagram of a nanoindentation experiment on a virus. The experiments can be carried out in air as well as in liquid. The minimal radius of curvature of commercial AFM tips is ~2–20 nm, a value that is, respectively, a little lower than or comparable to the size of small viruses. Before the start of a nanoindentation experiment, the viral particle needs to be imaged[102,103] to check whether it has the correct shape and size (Fig. B3a). Viral imaging under liquid conditions in combination with mechanical probing has been carried out in tapping-mode[104] and jumping-mode[105] AFM, two relatively non-invasive imaging modes, which is of importance for the imaging of fragile biological structures such as icosahedral viruses. The more rigid, rod-like viruses have been imaged in contact-mode AFM without inducing visible damage[69]. Imaging is followed by indentation of the virus, during which a force–distance curve (FZC) is recorded. This FZC involves the bending of two springs in series, the cantilever and the viral particle. For this reason, a calibration FZC of the cantilever deflection on the solid substrate next to the virus must be recorded. From these two FZCs the FDC of the virus can be determined, showing the force as a function of the indentation of the virus (Fig. B2b,d). The schematic FDC of Fig. B2d shows an initially linear deformation regime with positive slope, for forces up to 1.7 nN, that is fully reversible. The slope of a linear, reversible indentation curve yields the particle's 'spring constant' and Young's modulus, as discussed in the text. This is followed by a deformation regime with negative slope, which is usually irreversible. This drop in force can indicate buckling of the shell or fracture of the shell ('failure'). Figure B3 shows a viral particle before and after a nanoindentation experiment. A hole produced by shell failure is clearly visible. Note that individual capsomeres are discernible. By comparing the image before and after indentation, the capsomeres that were removed by the indentation can be identified.

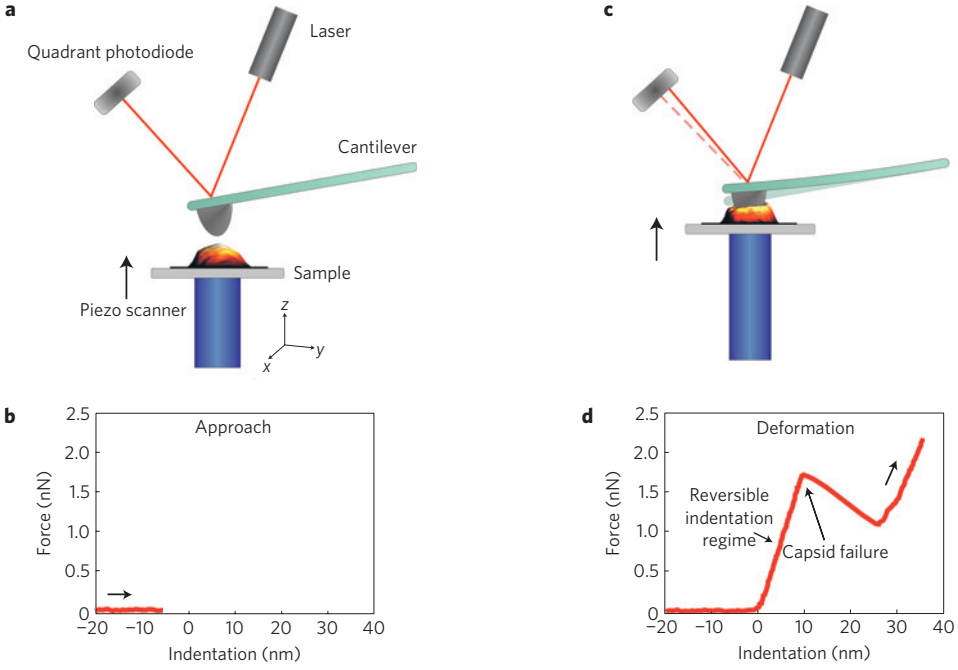

Figure B2 | Schematic diagram of AFM nanoindentation. a,**b**, The piezo is extending in **a**, but the AFM tip has not yet touched the virus surface and therefore the exerted force is zero (**b**). **c**,**d**, The AFM tip is indenting the virus and the cantilever bends (**c**); the change in signal on the quadrant photodiode is a measure for the exerted force, plotted in **d** as a function of the indentation.

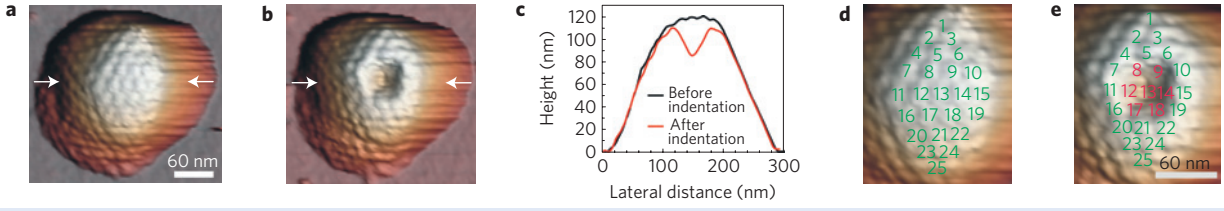

Figure B3 | AFM images of a single viral particle before and after nanoindentation. a,**b**, Three-dimensional rendered AFM topography images of a liquid-immersed HSV1 particle before (**a**) and after (**b**) indentation. The structural subunits (capsomeres) can be recognized on the viral shell. **c**, The height profile, taken along the white arrows in **a** and **b**, shows the capsomeres on top of the particle before indentation and the hole left after indentation. The indented profile most probably represents the tip shape and because of the finite width of the AFM tip it was not possible to image inside the broken capsid. **d**,**e**, Numbering of the capsomeres before and after indentation reveals the removal of seven (denoted in red) central capsomeres as a result of shell failure. Reproduced with permission from ref. 65, © 2009 NAS, USA.